Infrasound from hurricanes: Dependence on the ambient ocean surface wave field

Claus H. Hetzer,[1] Roger Waxler,[1] Kenneth E. Gilbert,[1] Carrick L. Talmadge,[1] and Henry E. Bass[1]

Received 7 May 2008; revised 12 June 2008; accepted 16 June 2008; published 29 July 2008.

[1] Infrasound signals in the microbarom band (about 0.2 Hz) generated by hurricanes often do not appear to originate near the eye where the winds are strongest. This paper suggests that conditions conducive to microbarom (and microseism) generation can occur along the trailing periphery of the storm through the interaction of the storm-generated wavefield with the ambient swell field, resulting in detection bearings that vary from the center of the storm by up to 20 degrees. Infrasound data from Typhoon Usagi (2007) is presented that supports this theory. **Citation:** Hetzer, C. H., R. Waxler, K. E. Gilbert, C. L. Talmadge, and H. E. Bass (2008), Infrasound from hurricanes: Dependence on the ambient ocean surface wave field, *Geophys. Res. Lett.*, *35*, L14609, doi:10.1029/2008GL034614.

1. Introduction

[2] The mechanism for generation of double-frequency microseisms (hereafter referred to as microseisms for simplicity unless specified otherwise) was presented by *Longuet-Higgins* [1950]. Similar acoustic signals in the atmosphere were named microbaroms by *Benioff and Gutenberg* [1939], and theories for their generation were developed by *Posmentier* [1967], *Brekhovskikh et al.* [1973], and *Waxler and Gilbert* [2006]. When ocean surface waves of the same frequency traveling in near-opposite directions interact, microbaroms and microseisms are produced at twice the frequency of the source waves through a nonlinear effect. Since the dominant ocean surface wave period is approximately 10 seconds (i.e. the frequency is 0.1 Hz), the dominant microbarom and microseism peak is at about 0.2 Hz. *Donn* [1951, 1952] applied this theory to seismic recordings made at Palisades, New York and related times of greater microseism energy to the presence of offshore storms, while *Donn and Naini* [1973] used signals from a storm to confirm that microseisms and microbaroms have a common source. More recently, the utility of using ambient noise such as microseisms and microbaroms for tomography of the earth [e.g., *Shapiro et al.*, 2005] and atmosphere [e.g., *Garcés et al.*, 2004] has demonstrated the need for more precise knowledge of their source regions. *Willis et al.* [2004] and *Kedar et al.* [2008] used the WaveWatch 3 ocean surface wave model of *Tolman et al.* [2002] to predict regions of possible strong infrasonic and seismic noise generation due to the interaction of surface waves, an idea that we also adopt for this paper.

[3] Microseisms were associated with cyclonic storms (i.e. hurricanes) as early as 1894 [*Deppermann*, 1951], and the link was confirmed by *Gilmore and Hubert* [1948], *Donn* [1952], and others. At first glance, it might be assumed that the microbarom source region associated with a hurricane would be coincident with the area of highest winds (the eye wall); this case was considered by *Longuet-Higgins* [1950], among others. *Cessaro* [1994], however, has shown that the association between a storm's trajectory and its associated microseism source is unfocused. More specifically, *Latham et al.* [1967], *Tabulevich* [1992], *Ponomaryov et al.* [1998], and *Willis et al.* [2004] found that the generation region for microseisms and/or microbarom-band infrasound is often observed to lag behind the storm eye, in its wake. An example of this can be seen in seismic records from Hurricane Fabian in 2003 (Figure 1). A spectrogram of the vertical seismic channel recorded at broadband station BBSR in Bermuda shows that the energy of the single-frequency microseism peaks on September 5, at the time of closest approach of the storm eye, while the double-frequency microseism peaks some 12 hours later, as the storm is departing (Figure 1). This effect is unrelated to the strength of the storm as wind speeds were decreasing during this time, suggesting that the proximity of a trailing source region is the cause for the intensity peak. This observation is in keeping with previous work [e.g., *Cessaro*, 1994] demonstrating that the single-frequency microseism is generated by shoaling of individual waves, while the double-frequency microseism is generated by wave-wave interaction.

[4] Hurricane wave models that might be used to determine the microbarom source region often consider only the waves generated by the storm itself [e.g., *Xu et al.*, 2007]. In these cases the potential for oppositely-directed waves is very small as the winds blow concentrically and the resultant ocean waves propagate in the same direction. However, in the case of a cyclonic storm located in an ocean basin with monodirectional ambient swell, it is obvious that there will always be a region where the dominant swell direction opposes the direction of the storm waves. This region will occur along the periphery of the storm, at the radius at which the storm-generated swell begins to overwhelm the ambient swell. Furthermore, in the case of (for example) Northern-hemisphere Pacific typhoons which travel to the northwest and have counterclockwise winds, the dominant summertime east-to-west swell will oppose the hurricane waves at a point behind the storm (for example, at about 15°N, 143°E on Figure 2). The output of Wave Action Models (WAMs), such as the WaveWatch 3 model [*Tolman et al.*, 2002], show both the storm-generated and ambient swell directions and can aid in the identifica-

[1]National Center for Physical Acoustics, University of Mississippi, University, Mississippi, USA.

0094-8276/08/2008GL034614

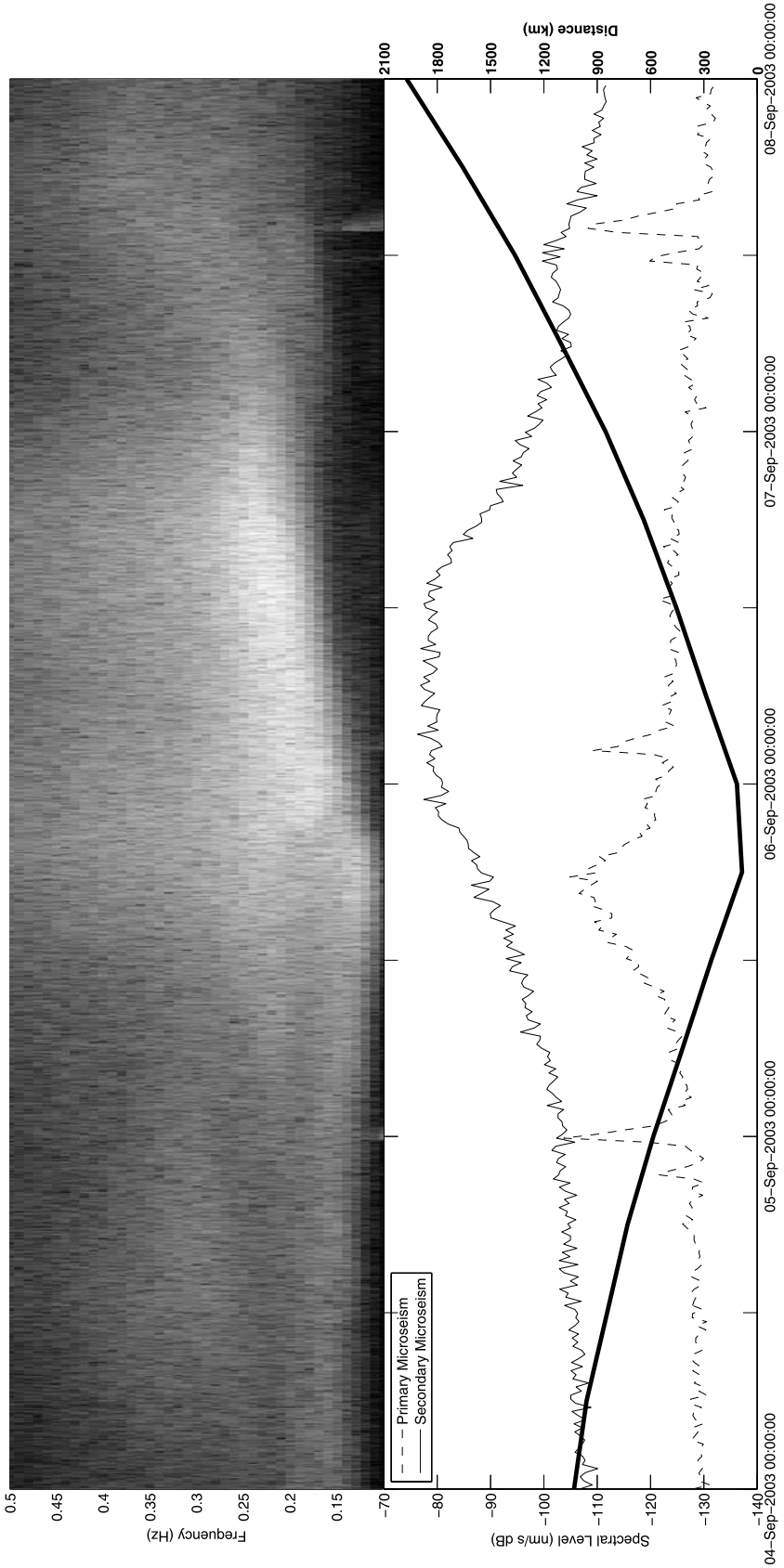

Figure 1. Spectrogram (top) and spectral levels for the primary (dashed) and secondary (solid, light) microseisms, and distance from eye (solid, heavy), as a function of time for Hurricane Fabian as recorded at seismic station BBSR, Bermuda (bottom). Spectrogram grayscale shows highest energy as white, lowest as black.

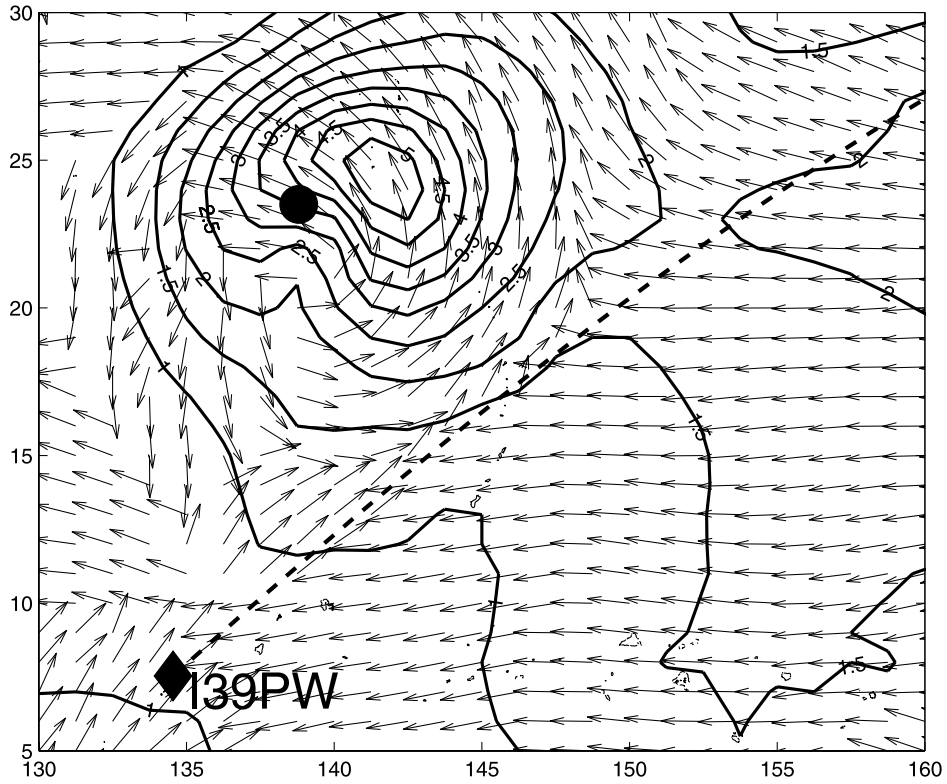

Figure 2. Significant wave height (contours, in meters) and dominant swell direction (arrows) for 31 July 2007, 12:00 UT. The solid circle indicates the eye position as reported by Unisys Weather (available at http://weather.unisys.com/hurricane/index.html). The heavy dashed line shows the bearing calculated for microbarom data recorded at infrasound array I39PW at this time. Wave vectors are rotated 180 degrees from reported to indicate the direction of propagation rather than the direction from which they arrive.

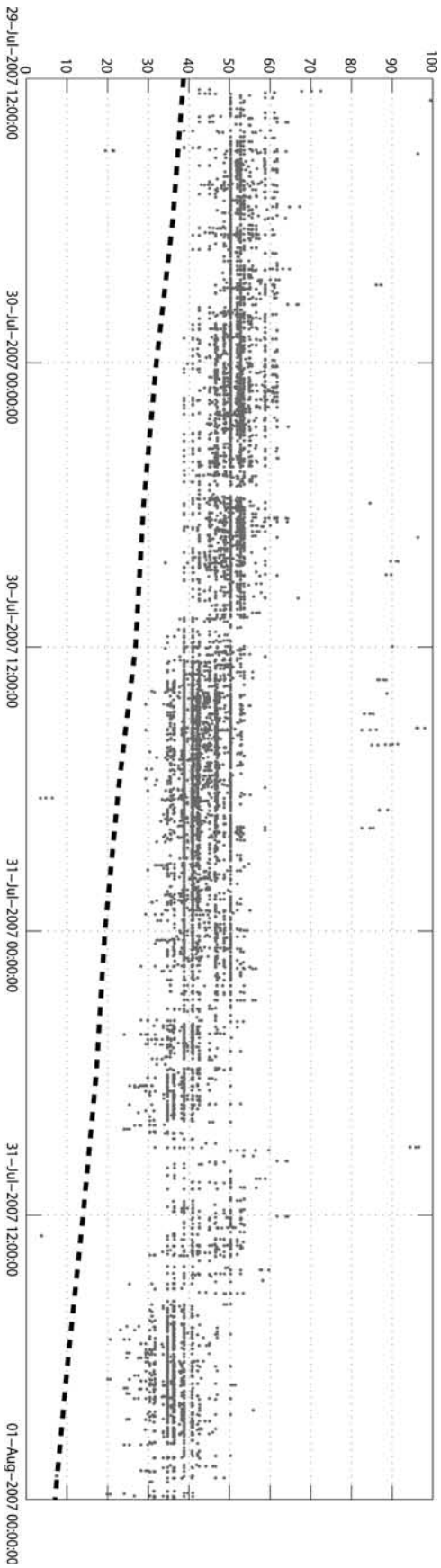

Figure 3. Calculated bearings (gray dots) for microbarom signals from Typhoon Usagi at I39PW, and the bearing to the reported storm eye location (dashed line) for 29–31 July 2007.

tion of such source regions. The full output of these models also contain the directional wave spectrum at every point on the specified global grid [*Willis et al.*, 2004; *Kedar et al.*, 2008], which can be used to directly calculate the opposing wave energy (and thereby source strength) as a function of period and direction. The utility of the full output, possibly on a finer-scale grid, will be investigated in future studies.

[5] The region of wave opposition in the surface wave field is analogous to the stagnation zone that forms when hurricane winds interact with the ambient wind field [*Willoughby et al.*, 1984, Figure 18]. The effect should be most simply observed in storms propagating through the open ocean and interacting minimally with reflections from continents; thus, island infrasound stations should be ideal locations from which to study this effect. Potential recording scenarios will, however, be limited by wind noise, proximity of other microbarom sources, and prevailing winds [*Garcés et al.*, 2004]. The effect has been observed, seismically, by *Chevrot et al.* [2007] related to an extratropical storm in the Mediterranean, but their scenario was more complicated due to shifting winds and nearby continental masses. We propose that the effect may be a dominant source for storm-generated microbaroms for deep-water hurricanes in the open ocean.

2. Supporting Observations

[6] In this paper we present infrasound recordings from one storm that support a hypothesis for microbarom generation by the interaction of hurricane-generated waves and the ambient swell field. Typhoon Usagi (2007) was recorded at infrasound station I39PW, Palau, which is among those installed as part of the International Monitoring System of the Comprehensive Nuclear-Test-Ban Treaty. I39PW records continuous infrasonic pressure data on a 7-instrument array at a 20-Hertz sample rate using Tekelec MB2000 microbarometers. The use of arrays for infrasound studies allows the azimuth of incoming arrivals to be directly calculated using correlation techniques. For this study the data were analyzed using the PMCC method [*Cansi*, 1995], a correlation-based technique commonly used in the infrasound community (A. Le Pichon and Y. Cansi, PMCC for infrasound data processing, Inframatics Newsletter, June 2003, available at http://www.inframatics.org).

[7] Typhoon Usagi was active in the Pacific basin from July 28 to August 3, 2007, reaching its peak intensity on August 1 as a Category 4 typhoon with winds at 120 knots. During this time it passed near the infrasound station I39PW at Palau (7.54°N, 134.55°E). Infrasound signals from Usagi became detectable at about 12:00 GMT on July 29 2007 and remained strong through August 1 (Figure 3). The detection azimuths are offset from the infrasound signals by roughly 20 degrees clockwise from north on average, that is, the bearings point behind the storm along its track. This offset is consistent throughout the entire time of detection. It is far too great to be explained by propagation time, and ray

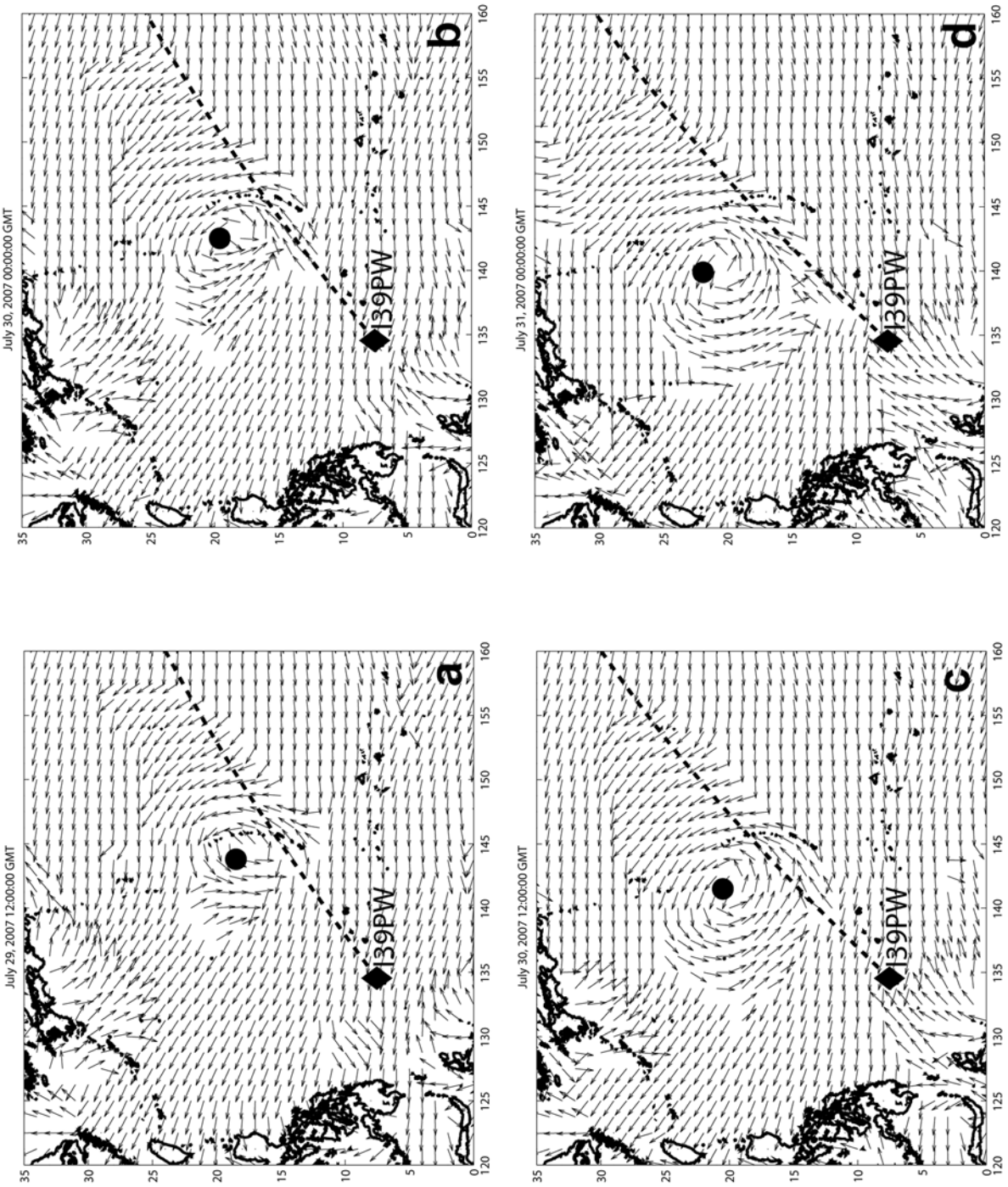

Figure 4. Surface wave hindcasts showing the storm-generated and ambient wavefields on (a) 29 July 2007 12:00 GMT, (b) 30 July 00:00 GMT, (c) 30 July 12:00 GMT, and (d) 31 July 00:00 GMT. The solid circle is the storm eye location and the heavy dashed line is the average bearing recorded at infrasound array I39PW at that time.

tracing through a hindcast atmospheric specification [*Garcés et al.*, 1998; *Drob et al.*, 2003] predicts crosswind deflection of only 2–3 degrees, ruling out propagation effects. We conclude, in agreement with previous work, that the generation region lies behind the storm.

[8] Examination of the dominant surface swell field using results archived by NOAA from their regular runs of the WaveWatch 3 model [*Tolman et al.*, 2002] show, as expected, a region along the southeastern periphery of the storm where the dominant ambient swell direction (toward the west) opposes the counterclockwise rotation of the storm swell (Figure 2). The infrasound bearing, shown by the heavy dashed black line, can be seen to point directly toward this region. The bearing offset is consistent throughout the time during which Usagi is observed, although scatter increases with time as Usagi gets farther away from the station (and closer to land). A series of wave hindcasts at 12-hour intervals as shown in Figure 4 demonstrates this consistency, as well as the continual tracking of the region of interaction.

3. Conclusions

[9] It has been observed that microbarom and microseism source regions often appear to trail the center of the storm. A physical explanation has been proposed that notes the potential for interaction between the concentric storm-generated wavefield and the ambient monodirectional swell. Infrasound data from Typhoon Usagi tracks a region that, according to surface-wave hindcasts, contains oppositely-directed ocean waves and trails the storm by a considerable distance. Seismic data from Hurricane Fabian also suggest, more indirectly, a microseism source that trails behind the main storm (and behind the source of single-frequency microseisms). This theory suggests that the interaction region for hurricane-generated waves and ambient swell, although certainly not the only potential source of hurricane microbaroms, provides an intuitive explanation for some prior and current observations, and is consistent with existing theories on microbarom generation. The application of the full WaveWatch 3 output to quantification of opposing-wave energy and direct calculation of hurricane microbarom source strength will be the subject of future studies.

[10] **Acknowledgments.** Maps generated using Generic Mapping Tools [*Wessel and Smith*, 1991]. Infrasound data from http://www.rdss.info. Seismic data from the Global Seismic Network operated by the USGS Albuquerque Seismological Laboratory.

References

Benioff, H., and B. Gutenberg (1939), Waves and currents recorded by electromagnetic barographs, *Bull. Am. Meteorol. Soc.*, *20*(10), 421–426.

Brekhovskikh, L. M., V. V. Goncharov, V. M. Kurtepov, and K. A. Naugolnykh (1973), The radiation of infrasound into the atmosphere by surface waves in the ocean, *Izv. Acad. Sci. USSR Atmos. Oceanic Phys., Engl. Transl.*, *9*(9), 899–907.

Cansi, Y. (1995), An automatic seismic event processing for detection and location: The P.M.C.C. method, *Geophys. Res. Lett.*, *22*(9), 1021–1024.

Cessaro, R. K. (1994), Sources of primary and secondary microseisms, *Bull. Seismol. Soc. Am.*, *84*(1), 142–148.

Chevrot, S., M. Sylvander, S. Benahmed, C. Ponsolles, J. M. Lefèvre, and D. Paradis (2007), Source locations of secondary microseisms in western Europe: Evidence for both coastal and pelagic sources, *J. Geophys. Res.*, *112*, B11301, doi:10.1029/2007JB005059.

Deppermann, C. E. (1951), Father Jose Algue, S. J., and microseisms, *Bull. Seismol. Soc. Am.*, *41*(4), 301–302.

Donn, W. L. (1951), Frontal microseisms generated in the western North Atlantic Ocean, *J. Meteorol.*, *9*, 406–415.

Donn, W. L. (1952), Cyclonic microseisms generated in the western North Atlantic Ocean, *J. Meteorol.*, *9*, 61–71.

Donn, W. L., and B. Naini (1973), Sea wave origin of microbaroms and microseisms, *J. Geophys. Res.*, *78*(21), 4482–4488.

Drob, D. P., J. M. Picone, and M. Garcés (2003), Global morphology of infrasound propagation, *J. Geophys. Res.*, *108*(D21), 4680, doi:10.1029/2002JD003307.

Garcés, M. A., K. G. Lindquist, and R. A. Hansen (1998), Traveltimes for infrasonic waves propagating in a stratified atmosphere, *Geophys. J. Int.*, *135*, 255–263.

Garcés, M., M. Willis, C. Hetzer, A. Le Pichon, and D. Drob (2004), On using ocean swells for continuous infrasonic measurements of winds and temperature in the lower, middle, and upper atmosphere, *Geophys. Res. Lett.*, *31*, L19304, doi:10.1029/2004GL020696.

Gilmore, M. H., and W. E. Hubert (1948), Microseisms and Pacific typhoons, *Bull. Seismol. Soc. Am.*, *38*, 195–228.

Kedar, S., M. Longuet-Higgins, F. Webb, N. Graham, R. Clayton, and C. Jones (2008), The origin of deep ocean microseisms in the North Atlantic Ocean, *Proc. R. Soc., Ser. A*, *464*, 777–793.

Latham, G. V., R. S. Anderson, and M. Ewing (1967), Pressure variations produced at the ocean bottom by hurricanes, *J. Geophys. Res.*, *72*(22), 5693–5704.

Longuet-Higgins, M. S. (1950), A theory on the origin of microseisms, *Philos. Trans. R. Soc. London, Ser. A*, *243*(857), 1–35.

Ponomaryov, E. A., A. G. Sorokin, and V. N. Tabulevich (1998), Microseisms and infrasound: A kind of remote sensing, *Phys. Earth Planet. Inter.*, *108*, 339–346.

Posmentier, E. S. (1967), A theory of microbaroms, *Geophys. J.R. Astron. Soc.*, *13*, 487–501.

Shapiro, N. M., M. Campillo, L. Stehly, and M. H. Ritzwoller (2005), High-resolution surface-wave tomography from ambient seismic noise, *Science*, *307*, 1615–1618.

Tabulevich, V. N. (1992), *Microseismic and Infrasound Waves*, in *Research Reports in Physics*, Springer, Berlin.

Tolman, H. L., B. Balasubramaniyan, L. D. Burroughs, D. V. Chalikov, Y. Y. Chao, H. S. Chen, and V. M. Gerald (2002), Development and implementation of wind-generated ocean surface wave models at NCEP, *Weather Forecasting*, *17*, 311–333.

Waxler, R., and K. E. Gilbert (2006), The radiation of atmospheric microbaroms by ocean waves, *J. Acoust. Soc. Am.*, *119*(5), 2651–2664.

Wessel, P., and W. H. F. Smith (1991), Free software helps map and display data, *Eos Trans. AGU*, *72*, 441.

Willis, M., M. Garcés, C. Hetzer, and S. Businger (2004), Infrasonic observations of open ocean swells in the Pacific: Deciphering the song of the sea, *Geophys. Res. Lett.*, *31*, L19303, doi:10.1029/2004GL020684.

Willoughby, H. E., F. D. Marks Jr, and R. J. Feinberg (1984), Stationary and moving convective bands in hurricanes, *J. Atmos. Sci.*, *41*(22), 3189–3211.

Xu, F., W. Perrie, B. Toulany, and P. C. Smith (2007), Wind-generated waves in Hurricane Juan, *Ocean Modell.*, *16*, 188–205.

H. E. Bass, K. E. Gilbert, C. H. Hetzer, C. L. Talmadge, and R. Waxler, National Center for Physical Acoustics, University of Mississippi, 1 Coliseum Drive, University, MS 38677, USA. (claus@olemiss.edu)